Journal of Hazardous Materials 506 (2026) 141579

Contents lists available at ScienceDirect

Journal of Hazardous Materials

journal homepage: www.elsevier.com/locate/jhazmat

Beyond size and shape: Physicochemical properties of microplastic test materials generated by cryomilling

Lucy Howarth-Forster [a,1,*], Robyn Barrett [a,1], Robert Clough [a], Lisbet Sørensen [b,c], Jack Allen [d], Chris Powell [d], Richard C. Thompson [e], Matthew Cole [f], Michael Wilde [a,*]

[a] School of Geography, Earth and Environmental Sciences, University of Plymouth, Plymouth PL4 8AA, UK
[b] Norwegian University of Science and Technology (NTNU), Department of Chemistry, Høgskoleringen, Trondheim 7491, Norway
[c] SINTEF Ocean AS, Department of Climate and Environment, Trondheim, Norway
[d] Centre for Sustainable Materials Processing, University of Leicester, Leicester LE1 7RH, UK
[e] School of Biological and Marine Sciences, University of Plymouth, Plymouth PL4 8AA, UK
[f] Marine Ecology & Society, Plymouth Marine Laboratory (PML), Plymouth PL1 3DH, UK

HIGHLIGHTS

- Size and morphology influenced by polymer material and milling parameters.
- Bulk polymer chemistry preserved during milling process.
- Cryomilling induced polymer-specific changes in crystallinity.
- Negligible contamination from plastic and metal milling components.

GRAPHICAL ABSTRACT

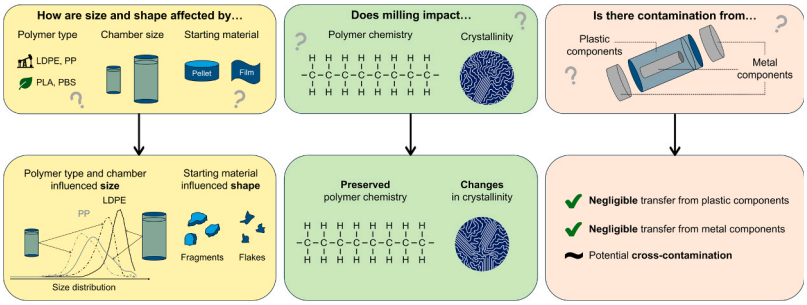

ARTICLE INFO

Keywords:
Microplastics
Test materials
Crystallinity
Contamination
Cryomilling

ABSTRACT

Cryomilling is a widely used method to generate microplastic test materials for environmental impact studies. To date, changes in physical, chemical and thermal properties, as well as potential contamination, in cryomilled materials have been inadequately assessed. Here, six polymer samples, including fossil-fuel based polymers (LDPE and PP) and bio-based polymers (PLA, PBS and a PLA/PBAT blend), were cryomilled with their physicochemical properties assessed before and after milling. Particle morphology was influenced by starting material form; pellets produced microplastic fragments whereas films produced thin flakes. Particle size distribution was polymer dependent but smaller size fractions were achieved by using a smaller milling chamber. Cryomilling retained bulk polymer chemical characteristics, including weathering-induced changes, indicating its suitability for generating microplastic test materials without significant alteration during processing. Contamination was negligible from both plastic and metal components of the milling apparatus, validating the use of cryomilled microplastics for leaching and ecotoxicological studies. While overall chemical integrity was preserved, cryomilling caused an increase in the degree of crystallinity in PP, PBS and PLA. These results provide crucial insight

* Corresponding authors.
E-mail addresses: lucy.howarth-forster@plymouth.ac.uk (L. Howarth-Forster), michael.wilde@plymouth.ac.uk (M. Wilde).
[1] These authors contributed equally to this work.

https://doi.org/10.1016/j.jhazmat.2026.141579
Received 26 August 2025; Received in revised form 12 November 2025; Accepted 20 February 2026
Available online 23 February 2026

into material properties, beyond size and shape, to better understand the influence of physicochemical properties on particle behaviour and draw meaningful associations between generated and environmental microplastics.

1. Introduction

Microplastics are recognised as globally important environmental contaminants, and are highly variable in polymer type, size, morphology, chemical composition and structural properties due to their diverse sources and environmental fate [1]. These physicochemical properties have a critical influence on the fate and impacts of microplastics in the environment, including particle transport dynamics [2]; deposition [3]; uptake by organisms [4]; potential toxicity [5]; adsorption [6]; leaching [7] and microbial colonisation [8].

To investigate the behaviour and effects of microplastic in the environment, appropriate test materials are required. Despite the observed heterogeneity of environmental microplastics, recent reviews have highlighted that the majority of microplastic effect studies rely on homogeneous, monodisperse commercially sourced particles, which potentially misrepresent the fate and impacts in the environment [9–12]. Out of 715 studies conducted between 2016 and 2020 on the impacts of microplastics, including toxicity, leaching, adsorption, and degradation, 63 % used uniform, industrially manufactured particles such as pellets or spheres [11]. Furthermore, over 89 % of studies focused solely on polystyrene (PS) and/or polyethylene (PE), highlighting the gap in research on the full range of polymer types, including bio-based and biodegradable plastics.

To address the need for more diverse test materials in experimental studies, methods for generating microplastic test materials from bulk plastics have been developed, including solubilisation and precipitation, ultrasonication, oxidative degradation, laser ablation and milling [13]. A particularly well adopted method to produce particles within the 1 μm−1 mm range is cryogenic milling, or cryomilling [14]. In fact, in the last year, several reference microplastics have become commercially available which were generated using cryomilling [15].

Cryomilling refers to the rapid cooling, typically using liquid nitrogen, and subsequent mechanical breakdown of a material. The technique has several advantages for microplastic generation. First, sample processing is relatively easy and there are a range of commercially available cryogenic mills including centrifugal mills, blade mills and impact driven mills. Secondly, the low temperatures embrittle the material [16], which means even tough plastics (e.g. PE) or elastomers (e.g. tyres), that are otherwise hard to grind, can be milled.

Given the growing adoption of cryomilling and cryomilled test materials in microplastic research, it is essential to understand whether the process may alter the material. While recent studies have primarily addressed size and shape changes induced by cryomilling, leading to the widespread assumption that cryomilling preserves chemical composition [17–19], evidence from other domains such as material science suggests that cryomilling may result in less apparent but potentially consequential chemical alterations including changes to thermal and structural properties (e.g. crystallinity) [20,21]. Additionally, the process of milling may introduce organic and metal chemical and particulate contaminants to the microplastic test material, but to date this has not been investigated. Substantial changes to material physicochemical properties, or the introduction of contaminants, may alter the behaviour of cryomilled microplastics in experimental studies. Without a comprehensive characterisation and understanding of all potential modifications, laboratory studies using cryomilled materials may misrepresent environmental processes, limiting the applicability of findings to real-world scenarios.

This study aimed to provide a comprehensive assessment of the impact of cryomilling on the physicochemical properties of plastic samples pre- and post-milling beyond size and shape. To achieve this, particle size and morphology alongside chemical composition and thermal properties were assessed. Microplastic test materials were generated from several polymer samples, including virgin pellets of low-density polyethylene (LDPE), polypropylene (PP), polylactic acid (PLA) and polybutylene succinate (PBS), as well as a commercially available agricultural mulch film. These samples represent conventional fossil-fuel-based thermoplastics, accounting for a third of global plastic production (PP: 19.0 %; LDPE: 14.0 % [22]), as well as bio-based and/or biodegradable polymers gaining popularity as sustainable alternatives to conventional plastics. Additionally, the mulch film represents a consumer product which, given its agricultural use, is intended to breakdown *in situ*. The results provide vital data to accurately interpret observations in environmental studies using microplastic test materials, and can be used to draw realistic comparisons between generated and environmental microplastics.

2. Methods

2.1. Plastic materials

Five virgin polymer samples were acquired in the form of pre-production pellets: PP (CAS #: 9003–07–0) and LDPE (CAS #: 9002–88–4) were obtained from Sigma-Aldrich, UK; PLA (CAS #: 26100–51–6) and a second LDPE sample (hereafter LDPE-STD) were purchased from Goodfellow Cambridge Ltd, UK; and PBS (CAS #: 25777–14–4) was gifted by PTT MCC Biochem Company Ltd, Thailand. Additionally, polyvinyl chloride (PVC, CAS #: 9002–86–2) was procured in granular form from Sigma-Aldrich, UK to serve as a reference for commercially available microplastic samples, not prepared via cryomilling. The granules were appropriate to use as a reference as they were similar in shape and morphology to other commercially available polymer materials used in microplastic studies [23–25]. A corresponding PVC sample for cryomilling could not be sourced at the time. The study focused on virgin products as these are primarily used as test materials, and pre-production pellets represent the second largest source of microplastics in the marine environment [26]. A final sample included a commercially available agricultural mulch film, comprising a polymer blend of PLA and polybutylene adipate terephthalate (PBAT). The mulch film was staked out with bamboo skewers in a private field, located in Cornwall (UK), and weathered for one month (June – July 2023), simulating the typical use case for the product. Regional weather conditions during the weathering period are given in Table S1.

2.2. Sample preparation

Polymer samples were cryomilled using a high-capacity freezer mill (Spex™ 6875 Freezer/Mill, UK) with liquid nitrogen. The accompanying polycarbonate (PC) milling chambers, equipped with stainless-steel end caps and impactor, were half-filled with plastic pellets and then milled according to the programmes outlined in Table S2. Where multiple runs were performed to mill a sample, the produced material was combined to reflect common practice in microplastic generation [18]. For PLA, the pellets resulted in the milling chambers cracking. Therefore, the pellets were first pressed into a film, using a 40-tonne hydraulic press (Bipel, Walsall, UK), which was then cut into ~1 cm^2 pieces to fill the milling chamber. The cracked chambers were discarded and replaced with new chambers. Polymers were milled in two different chamber sizes – large (product #: 6801, ~250 mL) and small (product #: 6751, ~25 mL) – with the exception of PLA and the mulch film which were milled in only the small and large chamber, respectively. This was due to limited sample amounts for PLA and the need to produce large quantities of the mulch film for use in a separate study. The influence on the size

distribution of microplastics produced by the different chamber sizes was investigated. Other milling parameters such as pre-cool time and the number of milling cycles were also tested, however these have been investigated elsewhere [27–29], and it was found that chamber size had the largest influence on particle size. Between each polymer sample, the milling chambers were washed with warm tap water and a detergent (Decon 90), as per the operating manual.

The microplastic samples generated from the virgin polymer samples were taken forward for analysis without any further processing to ensure a comprehensive analysis of the material. The mulch film was sieved, and the < 500 μm fraction retained for analysis, as this was part of a separate study. The samples were stored in dry, ambient conditions in glass sample jars which were cleaned using the same protocol as for the milling chambers.

2.3. Size, shape and morphology

2.3.1. Optical microscopy

Images of the original sample pellets and cryomilled particles were taken at × 0.6 and × 1 magnification using a stereomicroscope (Nikon, SMZ745T, Japan).

2.3.2. Scanning electron microscopy (SEM)

Scanning electron microscopy (SEM) was used to ascertain plastic particle size, shape and surface morphology after cryomilling. This was performed using a JEOL 7001 F (JEOL Ltd, Tokyo, Japan), in SE1 mode, maintaining an acceleration voltage of 15 kV and a 9–11 mm working distance. Samples were attached to stainless-steel stubs using double-sided carbon tape and sputter coated with palladium (K550X Sputter Coater, Quorum Technologies, UK). The sputter coating provides a 1–3 nm conductive layer on the non-conductive plastic sample, which reduces charge build-up on the sample and results in a higher image quality [30]. Images were taken for each sample at × 25, × 50 and × 150 magnification, with additional images at × 400 magnification for PP and PVC as these particles were smaller.

2.3.3. Particle size analysis (PSA) using laser diffraction

Particle size analysis (PSA) was performed using a Malvern Mastersizer (3000) laser diffraction instrument equipped with a Malvern Hydro LV dispersion unit (Malvern Panalytical Ltd, Malvern, UK). Samples were suspended in high purity water, with 5 % Terigtol added dropwise to reduce agglomeration during measurement. The suspension was then added to the dispersion unit until sufficient material was present to within the set obscuration limits. Measurement parameters of each polymer sample were optimised, after which five measurements for each subsample (n = 3) were taken. Measurements were taken in manual operation to allow for method optimisation and because manual cleaning was required between samples. Equivalent sphere diameters were measured, and the Mie theory was applied. The refractive index of each polymer was specified in the instrument parameters. Global instrument parameters and the results of the optimisation process are given in Tables S3-4.

2.4. Chemical analysis

2.4.1. Fourier-transform infrared spectroscopy (FTIR)

The polymers were analysed by Fourier-Transform Infrared spectroscopy (FTIR), using a Bruker Vertex 70 Spectrometer, with a diamond attenuated total reflection (ATR) attachment (Bruker, Billerica, MA, USA). Pellets and microplastic samples were measured in triplicate in transmittance mode with 32 scans in wavenumber range 400 – 4000 cm^{-1}. Spectra were analysed using OPUS software and compared to library matches.

2.4.2. Pyrolysis gas chromatography-mass spectrometry (Py-GC-MS)

Pyrolysis with gas chromatography coupled to mass spectrometry (Py-GC-MS) was performed with a Multi-Shot Pyrolyzer EGA/Py-3030D micro-furnace (Frontier Laboratories Ltd. Fukushima, Japan) coupled to a 7890 A Gas Chromatograph with a 5975 C Mass Detector (Agilent Technologies, Palo Alto, USA). An Ultra-Alloy-5 column (30 m x 0.25 mm x 0.25 μm, Frontier Laboratories Ltd.) was fitted in the GC.

Approximately, 70 – 100 μg of each sample were weighed into a stainless-steel ECO-cup and inserted into the microfurnace using an AS-1020E Auto-Shot sampler (Frontier Laboratories Ltd., Fukushima, Japan). Pellets and microplastic samples were measured in triplicate – for the pellets, small pieces were cut off using a stainless-steel craft knife to obtain the desired sample. Single-shot pyrolysis was performed at 600 °C for all samples as polymer breakage determined by evolved gas analysis (EGA) occurred below this temperature for all polymers [31–33].

The injection port operated at 300 °C, with a split ratio of 30:1, and the interface was maintained at 300 °C. Helium was used as the carrier gas, with a constant flow of 1 mL min^{-1}. The temperature programme was: 40 °C for 6 min; increasing to 310 °C at 20 °C min^{-1}; and finally an isothermal hold at 310 °C for 21 min. The detector operated in electron ionisation (EI) mode at 70 eV, and scanned in positive mode between 35 and 550 *m/z*. The ion source and quadrupole were held at 230 °C and 150 °C, respectively. All data were processed using Chromspace® (version 2.2, SepSolve) and the NIST Mass Spectral Search Program (version 2.4).

2.5. Thermal analysis

2.5.1. Thermogravimetric analysis with differential scanning calorimetry (TGA-DSC)

TGA-DSC was performed using a Mettler-Toledo TGA/DSC 1 with autosampler and STARe software. Both TGA and DSC were performed simultaneously on the same sample – TGA measures weight changes in a sample over a temperature ramp, while DSC measures heat flow within a sample as heat is applied. Considering the variability of DSC measurements, and limited instrument time for extensive repeat measurements, the measurements were made to capture key observable differences. Approximately 4 – 30 mg of each sample was placed into a 40 μL aluminium crucible (Mettler Toledo) and the temperature raised from 25 to 600 °C, at a heating rate of 10 °C min^{-1}, under nitrogen gas (purge and protective flows were both 100 mL min^{-1}). A 100 μL aluminium pan blank was used as the reference. The thermal profiles were plotted and interpreted using OriginPro® 2025 (OriginLab Corporation). The degree of crystallinity (X_c) was determined using Eq. 1, based on heat of fusion [34], where each sample's heat of fusion (ΔH_f, J g^{-1}) was calculated using Eq. 2 and compared to literature values of the corresponding 100 % crystalline polymer. See SI for literature values used for each polymer.

$$X_c = \frac{\Delta H_f}{\Delta H_f^0} \times 100 \quad (1)$$

$$\Delta H_f = \frac{\text{Area under the melting peak} \quad (W/g \quad .^\circ C)}{\text{Heating rate} \quad (^\circ C/s)} \quad (2)$$

2.6. Assessment of contamination

2.6.1. Plastic contamination

Fragments were observed to be coming off or stuck on to the inside of the PC milling chamber and these were isolated using metal forceps (referred to as 'inner' sample) and compared against samples of the milling tube acquired from the outside of the tube ('outer' sample). Fragments were analysed by ATR-FTIR and Py-GC-MS as described above. Additionally, the FTIR spectra and chromatograms of the original pellet and milled materials were analysed for indications of contamination.

2.6.2. Inductively coupled plasma mass spectrometry (ICP-MS)

The chamber caps and impactor in the freezer-mill were made of 440 C stainless-steel. Trace metal analysis was performed to assess whether any metal contamination was imparted during the milling procedure. It was expected that any metal contamination would be in low concentrations, therefore, for this analysis, the virgin polymer samples (LDPE, LDPE-STD, PP, PLA and PBS) and the corresponding microplastics generated in the small milling chambers were used. PLA samples included the film and pellet, and their corresponding milled forms. The mulch film was excluded because as a consumer product, and due to the additional weathering step the sample underwent, it was thought to have much higher metal concentrations which would occlude identification of small changes in metal concentrations caused by milling. PVC was also excluded as it was not milled.

A procedure adapted from Prunier *et al.* [35] was performed using a CEM Mars5 Xpress system, in which 50 – 100 mg of each polymer (n = 6) was solubilised in concentrated nitric acid (HNO_3, >68 %, trace metal grade, Fisher Scientific). Trace multi-elemental concentrations were subsequently measured on an inductively coupled plasma mass spectrometer (iCAP TQ ICP-MS, Thermo Fisher) which was checked for conformance with the manufacturers specifications before use, whilst EP-L certified reference material (CRM) was used to check the accuracy of the calibration standards. The elements of interest to assess for contamination were primarily iron (Fe) and chromium (Cr), given their high proportions within 440 C stainless-steel, as well as manganese (Mn) and molybdenum (Mo). Additionally, 17 other elements, shown in Table S9, were screened for since many different inorganics can be present in plastics [36]. Germanium, indium and iridium were used as internal standards. The ERM-EC680m (low-level) CRM was used to check the efficacy and repeatability of both the acid digestion and ICP-MS analyses. Blank samples exhibited low levels of aluminium contamination from the acid digestion procedure, but contamination was negligible for all other elements measured. The low levels of Al contamination were deemed to be acceptable, as it is not a component of stainless-steel. The recoveries of Cr and lead (Pb) from the ERM-EC680m were 97 % and 98 %, respectively, whereas the recovery of arsenic (As), antimony (Sb), tin (Sn) and zinc (Zn) were 79 %, 69 %, 53 % and 63 % respectively, suggesting the measured concentrations of the latter group of elements may be underestimated. The limit of detection (LOD) was determined as the average element concentration plus 3 times the standard deviation in measurements from the blank samples (n = 25).

2.7. Data analysis

All statistical analyses and data visualisations were carried out in R (R, version 4.2.2). *A priori* tests included Shapiro-Wilks and Levene's to determine normality and homogeneity of variance, respectively. All tested data was found to be non-parametric. A two-sample Kolmogorov-Smirnov test was applied to test for significant differences in particle size distributions between large and small chambers, as well as polymer specific responses to milling methods (as applicable). A directed Mann-Whitney *U* test was applied to assess if metal concentrations increased after milling for each polymer, with Holm's correction for multiple comparisons. All tests were carried out at 95 % significance level.

3. Results and discussion

3.1. Particle morphology influenced by starting material

Cryomilling produced heterogeneous particles for all polymer samples, as shown in the SEM and optical microscopy images (Fig. 1 and Figures S2-4), consistent with previous studies [15,16,37]. The pellets formed irregularly shaped fragments, whereas the PLA and mulch film formed flakes reflecting the original form of the material [38]. SEM analysis revealed that all the milled particles had a rough surface, with frayed and serrated edges, distinct from the purchased PVC microplastics, which were more homogeneous in size and shape with rounder edges. The PVC sample in this study was morphologically similar the 100 µm PVC particles characterised by Moura *et al.* [39], although from different suppliers.

Particle morphology affects microplastic transport through the environment [2], adsorption and leaching capacity [40] as well as toxicity [41,42]. Characterisation via SEM showed that starting material form influences the final microplastic morphology, so should be considered when creating microplastic test materials. It should also be noted that other morphologies, such as pellets and fibres, are also found

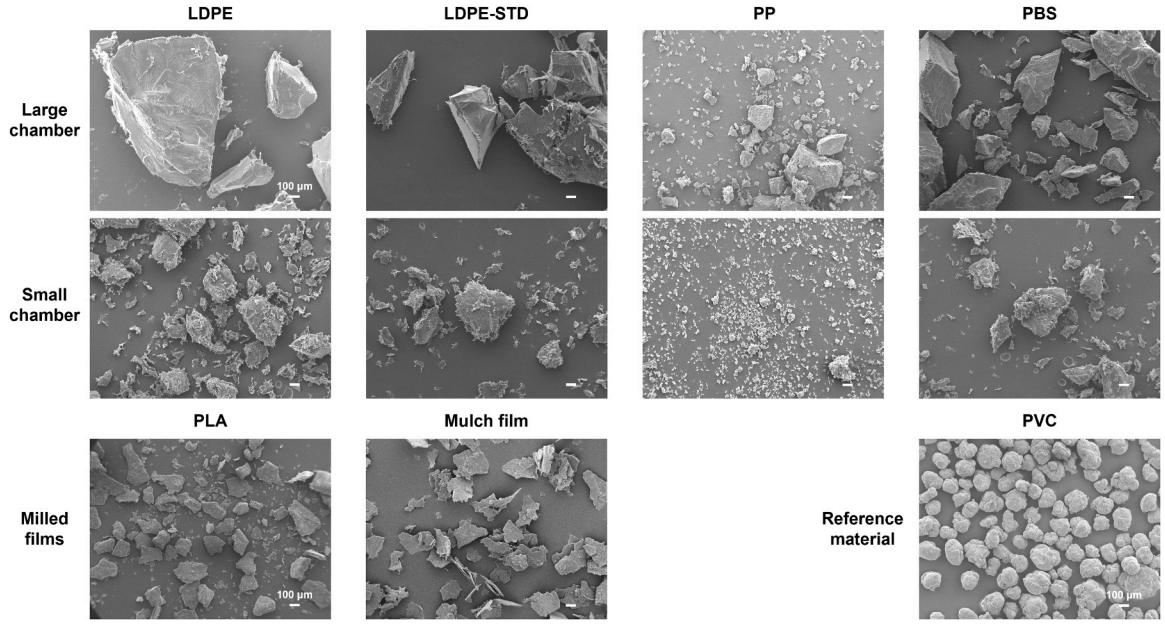

Fig. 1. SEM images of the cryomilled polymers, comparing the generated particles to a commercially available PVC reference material. Scale is the same for all images. For the LDPE, LDPE-STD, PP and PBS samples, images illustrate particles produced from the large chamber (top row) and small chamber (bottom row), as labelled. Note the different shapes produced from the pellets in comparison to the film samples, as well as the homogeneity of the commercially sourced PVC particles in comparison to those generated by cryomilling.

in the environment so test materials should be selected according to study aims. Furthermore, while the heterogeneous morphology of cryomilled particles is considered more representative of environmental plastic, cryomilling was not shown to reproduce surface characteristics such as pitting or pores which are generally observed in weathered plastic particles as a result of oxidation [43] or from microbial activity [44].

3.2. Polymer type and milling parameters influence particle size distribution

PSA showed the cryomilling procedures created a wide range of particle sizes; from < 10 μm (PP, small chamber) to over 1500 μm (LDPE and LDPE-STD, large chamber), all of which are within the accepted microplastic size range (<5 mm) observed in the environment (Fig. 2, Table S5). The milled samples had a broader size distribution than the PVC sample reflecting the homogeneity of the commercial particles. The mulch film had the narrowest size distribution of the milled samples, attributed to sieving the sample post-milling (Table S5). Sieving is often used after cryomilling to isolate desired size range of the test material, as required by the study.

There was a significant difference between the size of PP and LDPE milled in the large chamber (Kolmogorov-Smirnov, D = 0.27, p = 0.0014, Figure S5), demonstrating the influence of polymer type on size distribution, when milling methods are kept consistent. Similarly, Tewari *et al.* [45] found PP and PET produced distributions of 5–10 μm and 10–15 μm, respectively, under the same milling conditions. For all polymers, using a smaller milling chamber produced smaller particles, and this was statistically significant for the LDPE-STD sample (Kolmogorov-Smirnov, D = 0.2431, p = 0.0059, Figure S6). Previous work has achieved smaller size distributions by increasing milling time [17,27] or the number of milling cycles [28]. Interestingly, the LDPE-STD sample produced slightly larger particles in both chambers compared to the LDPE sample, despite having been milled for more cycles with a higher impactor rate. This could be due to physicochemical differences between the different LDPE samples or suggests cooling time has a greater influence on particle size than other milling parameters. Indeed, Eitzen *et al.* [46] increased the percentage of particles < 100 μm from 25 % to over 50 % by doubling the cooling time.

Particle size affects bioavailability [47,48], uptake and release of contaminants [49,50] and toxicity [7,51] and therefore is an important consideration for microplastic test materials. Cryomilling produced large quantities of test material, from a variety of polymers, within the size range of microplastics: 1 μm – 5 mm [41,52–54]. Particle size was influenced by polymer type as well as milling parameters, particularly chamber size. Therefore it is recommended that milling parameters are tailored to each polymer, as has been done in previous studies [55], and optimised for the target size range. For example, if targeting smaller size fractions, LDPE requires more milling cycles than PP and chamber size should be kept to a minimum. For use in further studies, sieving is recommended to ensure full control over particle size, excluding larger size fractions as needed and removing the smallest particles which may skew results [29]. Importantly, particle size should be thoroughly characterised to understand how size influences observed effects.

3.3. Polymer chemical properties are preserved during cryomilling

FTIR of each sample confirmed each polymer type. Despite the use of liquid nitrogen, cryomilling can induce mechanical degradation. However, adsorption peaks relating to polymer type showed little-to-no changes between the pellet and milled spectra (Figure S7-13). Furthermore, changes in polymer chemistry induced by weathering were preserved. Environmental exposure can lead to changes in polymer chemistry, visible by FTIR, such as an increase in oxygen containing functional groups [56]. This was seen in the mulch film sample, where a peak appeared at 1759 cm^{-1} in the weathered material, which was still apparent after the sample was cryomilled (Fig. 3).

A previous assessment of cryomilled PS by FTIR concluded cryomilling induced no change in surface chemistry [17]. However, FTIR analysis here of an expanded range of polymer materials, did reveal the presence and redistribution of surface additives. In both the large and small LDPE and LDPE-STD samples, and the PLA sample, additional peaks were observed in the spectra of the pellets which were not present in the corresponding milled material. In LDPE, peaks were observed at 3394 cm^{-1}, 3186 cm^{-1} and 1646 cm^{-1} (Fig. 4), characteristic of a primary amide group [57], and have been previously attributed to amine-based UV stabilisers present in LDPE [58]. Here, the observed signals were likely due to the presence of erucamide (reference spectra in Figure S14), a commonly used slip and anti-block agent in PE production [59], which the manufacturer reported the sample to contain. Erucamide is designed to migrate to the surface of polymers, where it is needed to reduce friction (slip agent) and prevent adhesion between

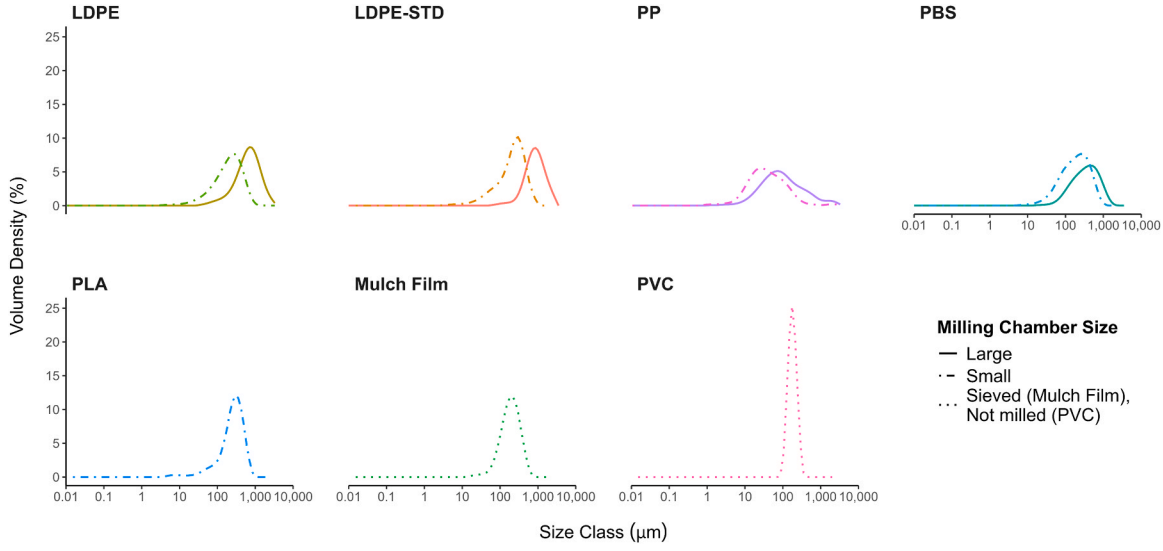

Fig. 2. Particle size analysis of the polymers milled compared to the commercially available PVC reference material. Note the logarithmic scale on the x-axis. The PVC sample has a much narrower size distribution compared to the cryomilled samples. For LDPE, LDPE-STD, PP and PBS, smaller size distributions were obtained by using a smaller milling chamber.

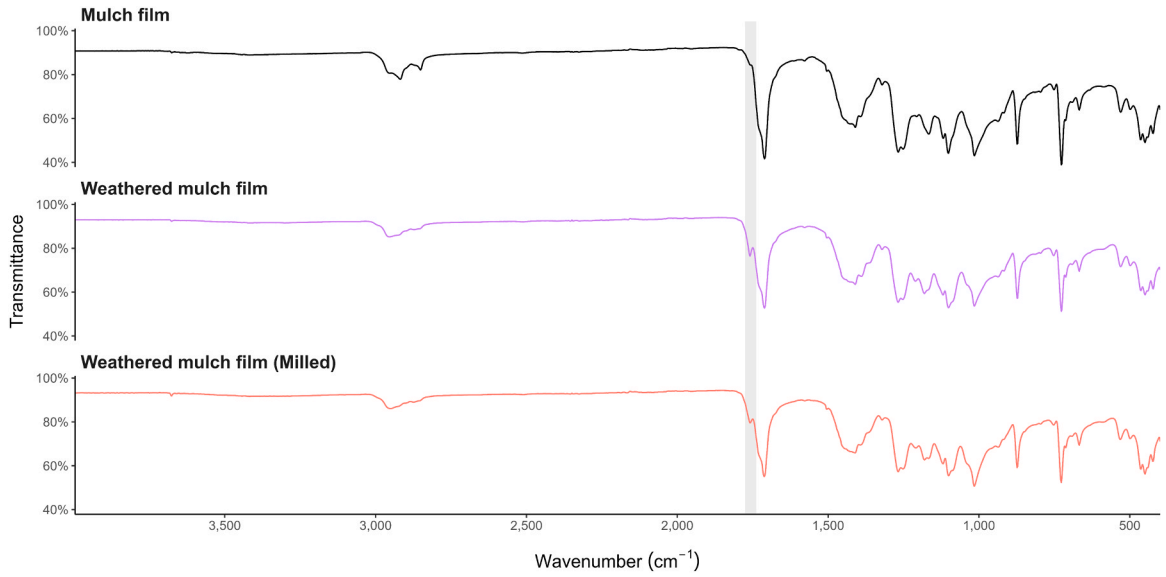

Fig. 3. FTIR spectra of as-received mulch film (top), weathered mulch film (middle) and milled weathered mulch film (bottom). Note the peak highlighted in the shaded area which appears after the mulch film was weathered and is still present in the milled sample.

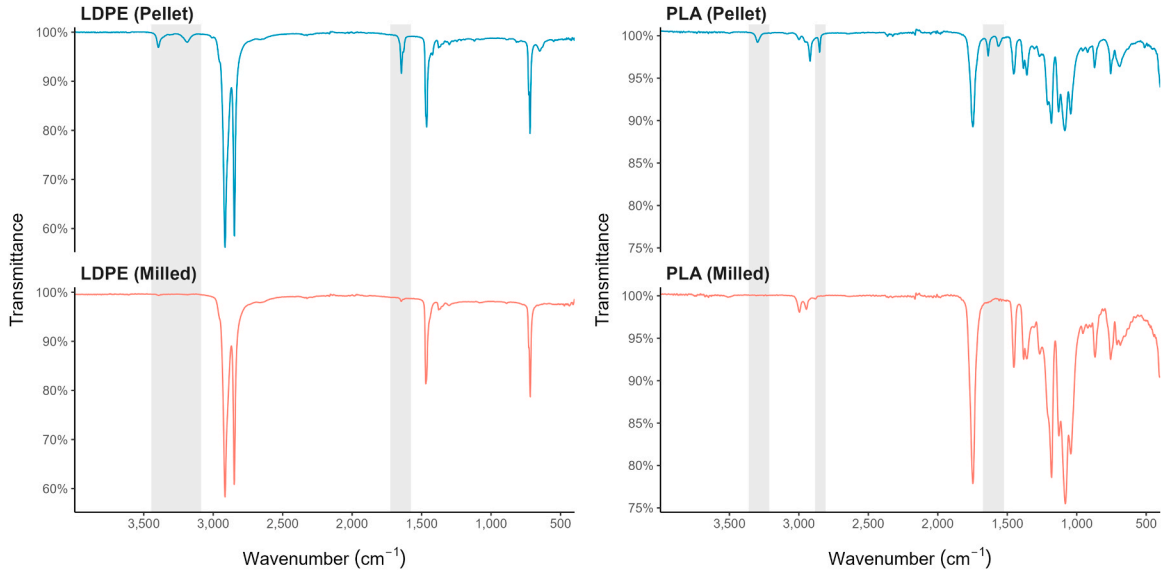

Fig. 4. FTIR spectra of pellet (top) and milled (bottom) samples of LDPE (left) and PLA (right). Additional peaks due to additive accumulation on the pellet surface are highlighted by shaded areas.

polymer layers (anti-block agent) and has been shown to crystallize there [60,61]. Therefore, once the pellet is milled and the internal polymer exposed, surface fragments which have accumulated erucamide are distributed throughout the milled sample, lowering the additive concentration below detectable limits. Similarly, the spectra for the PLA pellets had additional peaks at 3297 cm^{-1}, 2919 cm^{-1}, 2850 cm^{-1}, 1637 cm^{-1} and 1564 cm^{-1} (Fig. 4), attributed to the presence of a surface additive such as EFKA 5244, a nitrogen based wetting agent, or phosphoric acid trimethyl ester, a flame retardant (see Figures S15-16 for related FTIR spectra). The remaining samples had no observable difference between the pellet and milled spectra, either because they did not contain additive compounds, or any additives present were more evenly distributed throughout the material.

Py-GC-MS was used to analyse the bulk polymer sample, confirming polymer identity and supporting the FTIR analysis. Characteristic compounds used as markers for each of the polymers were identified (e.g. D, L-lactide dimer for PLA, and succinic anhydride for PBS) and the chromatograms reported (Figures S17-24). Comparison of chromatograms of the original material with that of the milled particles was performed using a pairwise probability-based subtraction (Smart Subtract, Chromspace®). The smart subtract tool is more powerful in identifying unique compounds in a sample over simple subtraction, as small relative differences in high intensity peaks are suppressed [62]. None of the samples showed any loss or gain of peaks in the milled samples compared to the original form.

Environmental microplastics often have complex chemical characteristics due to the presence of chemical additives, surface contaminants and environmental degradation [63]. Particle transport [64], chemical release [65,66] and toxicity [67,68] are influenced by particle chemistry, which includes bulk polymer composition as well as additional chemicals present. Particle chemistry also influences other physicochemical properties. For example, the introduction of

oxygen-containing functional groups enhances the hydrophilicity of microplastic particles, leading to increased adsorption of metals [69] and pharmaceuticals [70,71]. These chemical modifications also extend beyond simple adsorption processes. Liu *et al.* [72] demonstrated that surface-modified anionic nanoplastics form stable complexes with α-synuclein, whereas equivalent neutral and cationic surface-modified nanoplastics do not, highlighting how surface chemistry can govern specific molecular interactions. Therefore, it is important to understand the chemical properties of microplastic test materials before use in environmental studies.

Chemical analysis by FTIR and Py-GC-MS demonstrated that bulk polymer chemistry is preserved in cryomilling, including chemical changes induced by weathering. These results indicate that milling does not impact bulk composition, and that pre-processing steps, such as weathering, can be used to mimic environmental processes as the chemical features are preserved during milling. However, it should be noted that the weathered material used here was a thin mulch film, and cryomilling of larger, thicker, weathered materials may result in the distribution of weathering-induced surface changes as observed for surface additives. High concentrations of additives on the surface of the LDPE and PLA pellet samples were identified, but cryomilling appeared to redistribute surface-specific compounds. This suggests that surface characteristics are sensitive to cryomilling which should be considered when preparing microplastic test materials. This finding is relevant for leaching, bioavailability or toxicity studies. First, cryomilling may increase bioavailability of surface chemicals due to their redistribution throughout the sample, as well as the reduction in particle size. However, the results show that these chemicals were present at much lower concentrations in the milled material and therefore may not cause a toxicological effect. Second, it is important to understand what chemical compounds are present in the test material. This result shows it is necessary to characterise the test material after cryomilling, as results from characterisation of the pellet may lead to false assumptions that high levels of additive are present throughout the material. It is also recommended that a multi-technique approach is used for characterisation; here, FTIR exhibited good selectivity for detecting surface additives, whereas Py-GC-MS provided insight on the bulk polymer properties. Both methods herein were qualitative, however, when assessing the leaching or toxicity of additives where it is important to determine the exact amount of additional chemicals present, further quantitative characterisation using chemical extraction techniques may be necessary.

3.4. Cryomilling causes changes in crystallinity

TGA-DSC was used to identify changes in bulk material properties as a result of cryomilling. Thermal properties, such as melting temperature (T_m) and glass transition temperature (T_g), provide insight into structural properties such as crystallinity (X_c). The DSC profiles, as well as the TGA curve with the first weight derivative, for each polymer pre- and post-milling are shown in Fig. 5 and in the SI (Figures S25-30), respectively. Table S7 and S8 also denote values calculated from the TGA-DSC analysis.

Most dramatically, the DSC curves revealed the inversion of the expected endothermic degradation peaks for both LDPE pellet samples (Fig. 5). Chemical analysis identified the pellet surface as a hotspot for surface-migrating additives, which introduce sites facilitating oxidative degradation (exothermic process) of the polymer. The migration and degradation of erucamide at low temperatures (55 °C) or during storage can form carbonyl- and amide- containing species, has been shown to influence thermal behaviour of LDPE [73,74]. The exothermic peaks in the LDPE pellet samples corroborate the FTIR results and show the presence of high concentrations of additives at the pellet surface which is then dispersed throughout the cryomilled sample. Interestingly, exothermic degradation was also observed in the PP pellet sample. Similarly to LDPE, this indicates the presence of an additive or contaminant such as adsorbed or absorbed solvent, or moisture within the PP sample. This is supported by the TGA analysis, where a smaller peak is observed before the complete degradation of PP (Figure S27). However, the presence of an additive or contaminant was not observed in the FT-IR or Py-GC-MS of the PP sample, highlighting the importance of a multi-technique approach to analysis.

PLA in pellet, film and milled forms displayed similar TGA and DSC profiles, but the degree of crystallinity (X_c) was considerably different (Table S8). The PLA pellet's relatively high X_c (35 %) reflects well-developed crystalline domains typical of unprocessed material, while the film's lower crystallinity (11 %) suggests limited crystal growth during cooling, resulting in a more amorphous, flexible structure. The cryomilled PLA, produced from the film, exhibited an intermediate crystallinity of 25 %, potentially indicating that milling either

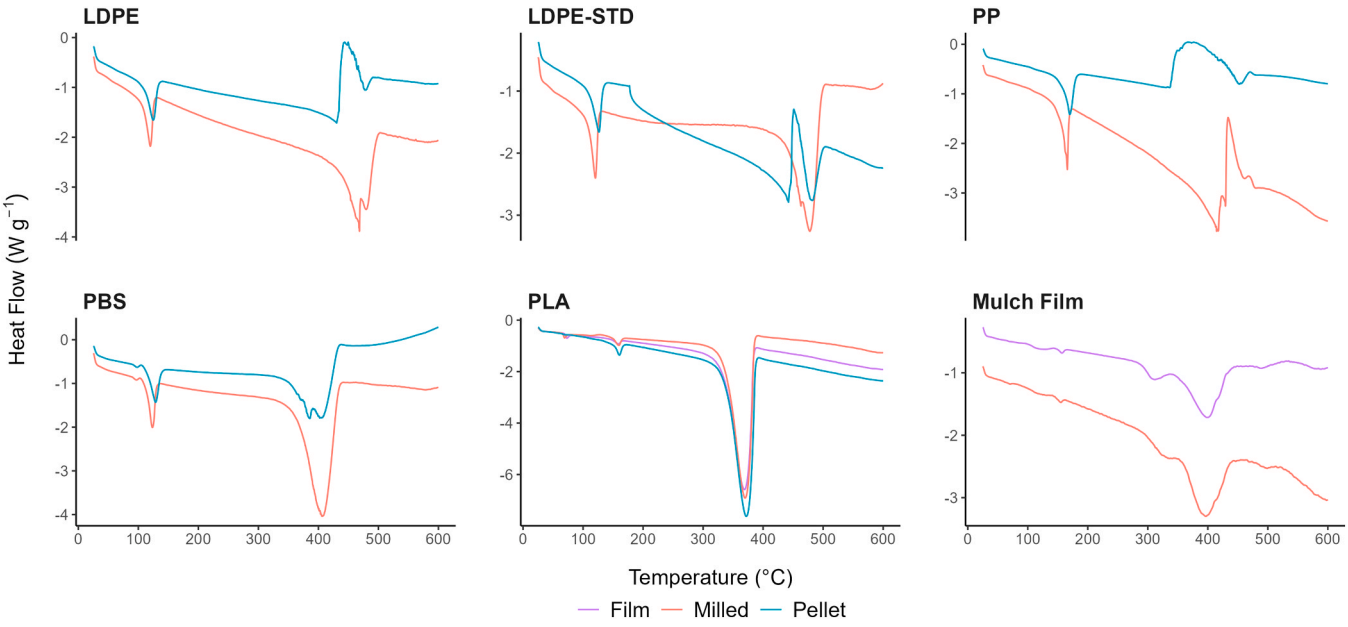

Fig. 5. DSC plots of the original and milled samples. Endothermic is down. Note the exothermic peaks in the LDPE, LDPE-STD and PP pellet samples – likely due to the presence of surface additives or contamination.

homogenised the film's non-uniform crystalline distribution or exposed pre-existing localised crystalline regions through mechanical disruption and enhanced chain mobility, as observed in similar studies [75,76].

The mulch film presented the most complex DSC and TGA profiles, showing a two-step degradation profile (Fig. 5 and Figure S30), corresponding to the blend of PLA and PBAT. At 500 °C, the mulch film had a 37.5 % weight residue, compared to < 2 % in the virgin samples, likely due to inorganic ash, metal oxides or other thermally stable components used to enhance material properties and reduce production costs [77], typical of consumer products. Comparison of the film and milled sample identifies a shift in the first degradation peak, attributed to PLA, while the PBAT-associated peak remains unchanged. This suggests the milling process selectively influenced the PLA component, possibly due to its greater susceptibility to mechanical disruption compared to the more ductile PBAT [78]. Alternatively, the shift in PLA degradation behaviour may be attributed to morphological changes within the blend. Cryomilling has likely disrupted the PLA and PBAT phase domains, resulting in a finer, more uniform dispersion of the polymers [79]. The increased interfacial area between PLA and PBAT can enhance heat transfer and potentially alter the local degradation environment of PLA, leading to the earlier onset of thermal degradation observed in the TGA [80].

The TGA-DSC analysis revealed substantial changes between pre- and post-milled samples, underscoring the impact of milling on polymer structure. Ducoli *et al.* [81] also reported milling-induced changes to the crystallinity of nano-sized PET and PA, using TGA and FTIR. Lionetto *et al.* [82] similarly reported increased amorphous content in PET nanoparticles during mechanical grinding, as confirmed by x-ray diffraction (XRD) and DSC. The extent of crystallinity change has been shown to depend not only on polymer type but also on the milling method. Ducoli *et al.* [83] found that ball milling induced the most pronounced changes to crystallinity, compared to centrifugal milling and immersion blending. Cuthbertson *et al.* [84] further demonstrated that cryomilling altered crystallinity across different polymers using TGA and DSC, with small-angle and wide-angle X-ray scattering (SAXS, WAXS).

Collectively, these results challenge the assumption that cryogenic milling of polymers at temperatures below their glass transition temperature preserves all material properties. While chemical integrity may remain largely unaffected, these studies demonstrate that crystallinity is highly susceptible to mechanical processing. The degree of crystallinity (Table S8) for PP was found to decrease after milling, whereas PLA appeared to regain crystallinity. This variability underscores the importance of considering polymer type and milling conditions when preparing laboratory-generated microplastics used to mimic environmental processes.

In the environment, secondary microplastics often exhibit increased crystallinity, as amorphous regions of plastics are more susceptible to oxidation, UV degradation and hydrolysis, leading to the reduction in those domains [85,86]. A study comparing raw polymers to weathered plastics collected from the North Atlantic sub-tropical gyre, reported that raw PE samples exhibited an average crystallinity of 42 %, while weathered microplastics showed an average of 54 % crystallinity [87]. The determined crystallinities of the cryomilled microplastics generated in this study (25–68 %) are consistent with environmentally weathered microplastics. The degree of crystallinity has a direct influence on microplastic behaviour and impact. For example, lower crystallinity enhances the adsorption capacity for hydrophobic pollutants [88] and increases additive and residual monomer mobility, thereby, increasing leaching potential [89], and bioavailability of potentially harmful substances. For example, a study reported that the leaching of Irganox 1010, a food additive, was inversely influenced by the crystallinity of the high-density polyethylene (HDPE) packaging. The lowest crystallinity material (51.6 %) demonstrated a partition coeffient (K) of 0.26, whereas the highest crystallinity sample (70 %) had a K value of 0.85. Therefore, as crystallinity increases, the K value or the amount of additive that remains in the material also increases and therefore leaching decreases [90]. Furthermore, studies have demonstrated that as the degree of crystallinity increases, enzymatic and hydrolytic degradation rates of polylactic acid decrease. Mechanistically, amorphous regions are more accessible to water and enzymes, while more crystalline samples prove more resistant to attack, retaining their integrity and consequently exhibiting lower degradation rates [91,92]. Therefore, comprehensive characterisation of thermal and structural properties of microplastic test materials, and consideration of how processing steps may alter these characteristics, is essential for future environmental impact studies.

3.5. Minimal contamination from cryomilling

3.5.1. Plastic contamination

Polycarbonate (PC) tubes make up part of the milling chambers used in the SPEX Freezer/Mill. PC is formed from the polymerization of bisphenol-A (BPA), a known endocrine disruptor [93,94]. After several rounds of cryomilling, wear and tear was visible on the inside of the PC milling chambers, with small plastic fragments detaching from the tube wall (see Figure S1-E). Therefore, it is important to assure that contamination from milling equipment is negligible before test materials are taken forward for toxicological or other studies.

The FTIR spectrum of two samples from the polycarbonate tube are given in Fig. 6. Interestingly, the inner tube sample spectrum matched the PLA library spectrum, as well as the PLA samples in this study. The outer tube sample showed characteristic peaks of PC, and a strong match to the PC library spectrum. The results identified the presence of polymer residues left after cryomilling and therefore the potential for cross-contamination of and between samples. Further analysis of the bulk material was performed using Py-GC-MS to determine if the inner tube sample was consistent with PLA or originated from the tube wall itself.

The chromatograms of the polycarbonate tube samples are given in Fig. 6. Again, the inner and outer sample do not match. The inner sample resembles the PLA chromatogram, and contains specific markers for PLA, while the outer sample chromatogram contains polycarbonate thermal degradation products: phenol; substituted phenols and the BPA monomer [95].

Extracted ion chromatograms (EICs) of the higher molecular weight degradation products, 4-(1-methyl-1phenylethyl)-phenol (m/z 197, 212) and BPA (m/z 213, 228) revealed no evidence of the polycarbonate markers. Further EICs were performed to assess for contamination from PC or PLA in all the milled samples, except PLA. Markers used for PLA were 2,3-pentanedione (m/z 43, 100) and 3,6-dimethyl-1,4-dioxane-2,5-dione (DL-Lactide, m/z 56, 144) (Figure S32-33). The EICs showed no evidence of contamination by neither PC nor PLA markers in the milled samples.

FTIR and Py-GC-MS analysis indicated no evidence of PC contamination from the milling tube. PLA was shown to adhere to the inner wall of the milling chamber, but was not detected in any of the other milled polymer samples. Similarly, comparative analysis of the FTIR spectra and Py-GC-MS chromatograms between non-milled and milled samples do not identify the introduction of contamination from other polymers. However, the abrasion on the inside of the tube means that cross-contamination from previously milled samples remains a concern. It is recommended that dedicated tubes are used for each sample or polymer type to mitigate this issue.

3.5.2. Metal contamination

The metal components of the milling chamber are made of 440 C stainless-steel – the elemental composition of which is given in Table S9. For use in cryomilling, 440 C has several desirable characteristics: it has high strength and hardness; it is magnetic (so can perform the oscillations necessary to break up the material) and is resistant to corrosion. However, it is possible that small amounts of metal are transferred to the milled plastics which could then influence subsequent experiments, such as ecotoxicological testing.

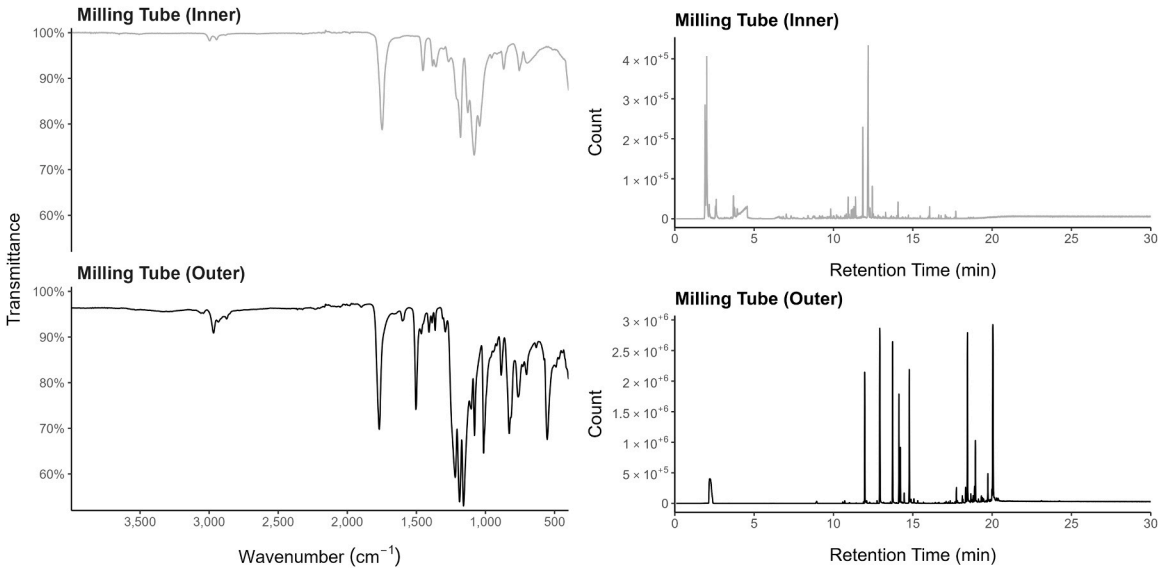

Fig. 6. Chemical analysis of the inner and outer portions of the milling tube. FTIR spectra (left) and Py-GC-MS chromatograms (right).

Elemental analysis revealed that three of the plastic samples contained trace levels of metals in both the pellets and milled material (Table S10): PBS contained titanium (Ti, 53.04 ± 5.81 μg g^{-1}), PP contained aluminium (Al) and Ti (55.18 ± 1.87 and 3.22 ± 0.31 μg g^{-1}, respectively), and PLA contained tin (Sn, 47.83 ± 6.09 μg g^{-1}). These elements are likely catalyst residue left over from polymerisation processes; titanium oxides are used to catalyse PBS formation [96–98], Ti and Al based Ziegler-Natta catalyst systems are often used in the synthesis of polyolefins such as polypropylene [99], and tin octoate (II) is a popular catalyst in PLA production [100]. Similar metal concentrations have been found in other studies. Peng *et al.* [101] reported 20.2 – 42.1 μg g^{-1} Sn in virgin PLA samples, and Eriksen *et al.* [102] reported 46 – 183 μg g^{-1} of Al and 2.5 – 5.5 μg g^{-1} Ti in virgin PP samples. However, this is the first report of trace metal concentrations in virgin PBS.

Results of the analysis of stainless-steel components in the samples are shown in Fig. 7. In the pre-milled samples concentrations of Cr were below the LOD, but there were low levels of Fe in the LDPE-STD, PLA and PP pellets as well as the PLA film, with a maximum concentration of 7.12 μg g^{-1} (PLA pellet). In comparison, the milled samples had detectable levels of Fe in at least one sample and at much higher concentrations, of up to 23.40 μg g^{-1} (PLA milled pellet). In most cases, when Fe was present in milled samples, Cr was also present. Statistical analysis found that metal concentrations between pre-milled and milled samples were not significant for all elements across all polymer samples (Mann-Whitney U, $p > 0.05$, Figure S35).

Other potential sources of contamination were also identified. The PLA film and corresponding milled sample contained detectable levels of lead (Pb) which were not found in the original PLA pellets and a sample of milled pellet recovered from a cracked chamber – suggesting contamination from the film making process. The presence of Fe detected in some pre-milled samples may indicate contamination from other metal equipment, such as metal spatulas used to transfer samples.

The concentration of stainless-steel elements in the samples remained below 0.0001 % wt in pre- and post-milled samples. Analysis of 59 milled virgin polymers using ICP-MS, by Cuthbertson *et al.* [84], identified low levels of metals, including Cr in a PC and an acrylonitrile butadiene styrene (ABS) sample at 0.005 % and 0.012 % wt, respectively. Parker *et al.* [103] identified stainless-steel elements, as well as zirconium (Zr) and yttrium (Y), by X-ray fluorescence (XRF) in milled PP and PVC which they attributed to their two-stage milling procedure – using a centrifugal mill with stainless-steel parts, followed by ball

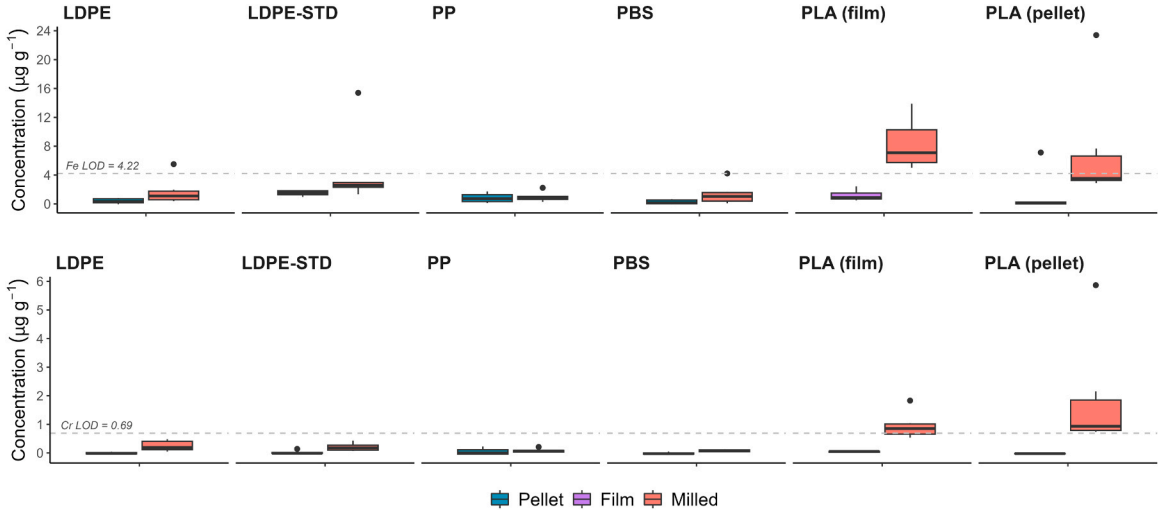

Fig. 7. Iron (top) and chromium (bottom) concentrations in non-milled and milled samples. The limit of detection (LOD) is shown by the grey dashed lines.

milling with Y-stabilised ZrO_2 balls. However, neither study reported the metal concentrations in the original polymer material.

Elemental analysis demonstrated that metal contamination can occur during milling. However, metal concentrations in the plastics themselves were more substantial than any transfer from the metal components of the milling apparatus, even in virgin polymer samples (Figure S34). Therefore metals inherent to the polymer from the manufacturing process are more likely to have greater influence over impacts such as toxicity. This effect would be magnified in consumer or post-consumer products which are likely to contain high concentrations of metals, for example, tyre particles contain high levels of zinc (Zn) [104,105]. Furthermore, environmental plastics are known to adsorb metals from the environment [106]. Kühn *et al.* [16] detected 31 elements in their marine litter mix, recording concentrations of Fe and Cr as high as ~1835 μg g^{-1} and ~179 μg g^{-1}, respectively. Therefore, it is concluded that contamination from the milling procedure used in this study will have negligible influence on further studies using the generated microplastics and validates the use of cryomilling to produce microplastic test materials.

3.6. Conclusion

Given the increasing use of cryomilling for the generation of microplastic test materials, this study aimed to characterise polymer samples before and after milling to identify material changes which may influence their behaviour in laboratory studies. SEM and PSA confirmed that cryomilling generated microplastics with irregular shapes and a broad size distribution. Particle shape was influenced by starting material form, and particle size distribution was dependent on polymer type but could be tailored by changing milling parameters such as chamber size and milling and cooling time. Bulk chemical properties, analysed by Py-GC-MS, were preserved in the cryomilling process, and FTIR demonstrated that milling served to homogenise the sample by redistributing additives which migrated to the surface of the initial plastic pellets. Thermal analysis by TGA-DSC also showed minimal changes in thermal properties, but indicated changes in crystallinity occurred during cryomilling, which were polymer dependent. Although few studies have explored the impact of structural properties on the behaviour of microplastics in the environment, it is thought to influence the formation of biofilm and is a key driver of chemical leaching. Contamination from plastic and metal components of the milling apparatus was negligible, however cross-contamination of plastic samples between milling is possible. A potential limitation of this study was the focus on virgin polymers and a weathered consumer product. Future studies incorporating marine-weathered and diverse post-consumer plastics, as well as investigations examining how milling-induced alterations influence toxicity endpoints, will help to establish whether cryomilled materials accurately represent the biological behaviour of environmentally relevant microplastics. Overall, cryomilling is shown to be a valid method for generating test materials, but the results identified material properties which are altered in the process. The comprehensive characterisation provides vital data of physicochemical properties, beyond size and shape, which influence material behaviour and allow for more realistic comparisons to be drawn between generated materials and environmental microplastics.

Environmental implication

Microplastics are known environmental contaminants, however their behaviour and impact are not fully understood. Cryomilling is used to replicate environmental microplastics – often assuming milling does not alter material properties or introduce contamination. This work tests these assumptions showing that contamination from milling is negligible and bulk polymer chemistry is preserved, but surface-specific characteristics are redistributed throughout the milled material and polymer-specific structural changes are induced by milling. These properties influence the behaviour and impact of microplastics. The data provided facilitates comparison between generated and environmental microplastics, making environmental studies which use cryomilled test materials more pertinent.

Funding

This work has received funding from the Natural Environment Research Council (NERC) through United Kingdom Research and Innovation (UKRI) for the Centre of Doctoral Training in Sustainable Management of UK Marine Resources (CDT SuMMeR) under grant agreement NE/W007215/1. Cole, Wilde and Thompson acknowledge funding from the Natural Environmental Research Council project "BioRisk" (NE/V007351/1). Wilde was also supported by the Community for Analytical Measurement Science through a 2021 CAMS Lectureship Award funded by the Analytical Chemistry Trust Fund.

CRediT authorship contribution statement

Matthew Cole: Writing – review & editing, Supervision. **Michael Wilde:** Writing – review & editing, Writing – original draft, Supervision, Methodology, Funding acquisition, Conceptualization. **Chris Powell:** Writing – review & editing, Methodology, Formal analysis. **Richard C. Thompson:** Writing – review & editing, Supervision, Funding acquisition. **Jack Allen:** Writing – review & editing, Methodology, Formal analysis. **Robert Clough:** Writing – review & editing, Methodology, Formal analysis. **Lisbet Sørensen:** Writing – review & editing, Supervision. **Lucy Howarth-Forster:** Writing – review & editing, Writing – original draft, Visualization, Methodology, Investigation, Formal analysis, Data curation, Conceptualization. **Robyn Barrett:** Writing – review & editing, Writing – original draft, Visualization, Methodology, Investigation, Formal analysis, Data curation, Conceptualization.

Declaration of Competing Interest

The authors declare that they have no known competing financial interests or personal relationships that could have appeared to influence the work reported in this paper.

Acknowledgements

The authors gratefully acknowledge the Plymouth Electron Microscopy Centre (PEMC, Plymouth, UK) for the support and assistance with the scanning electron microscopy. Billy Simmonds is thanked for the use of FTIR and ICP-MS and Richard Hartley for the use and help with analysis for particle size analysis. Dr Rachel Coppock for the preparation of the milled mulch film sample. Additionally, the authors thank Laura McGregor (SepSolve, Peterborough, UK) for the beta Chromspace software used for Py-GC-MS data analysis.

Appendix A. Supporting information

Supplementary data associated with this article can be found in the online version at doi:10.1016/j.jhazmat.2026.141579.

Data availability

Data will be made available on request.

References

[1] Li, W., et al., 2023. Sources, distribution, and environmental effects of microplastics: a systematic review. RSC Adv 13 (23), 15566–15574.
[2] McIlwraith, H.K., et al., 2024. Microplastic shape influences fate in vegetated wetlands. Environ Pollut 345, 123492.
[3] Du, S., et al., 2021. Environmental fate and impacts of microplastics in aquatic ecosystems: a review. RSC Adv 11 (26), 15762–15784.

[4] Botterell, Z.L.R., et al., 2020. Bioavailability of microplastics to marine zooplankton: effect of shape and infochemicals. Environ Sci Technol 54 (19), 12024–12033.
[5] Cole, M., et al., 2019. Effects of nylon microplastic on feeding, lipid accumulation, and moulting in a coldwater copepod. Environ Sci Technol 53 (12), 7075–7082.
[6] Guo, X., Wang, J., 2019. The chemical behaviors of microplastics in marine environment: a review. Mar Pollut Bull 142, 1–14.
[7] Gulizia, A.M., et al., 2023. Understanding plasticiser leaching from polystyrene microplastics. Sci Total Environ 857 (Pt 1), 159099.
[8] Hossain, M.R., et al., 2019. Microplastic surface properties affect bacterial colonization in freshwater. J Basic Microbiol 59 (1), 54–61.
[9] de Ruijter, V.N., et al., 2020. Quality criteria for microplastic effect studies in the context of risk assessment: a critical review. Environ Sci Technol 54 (19), 11692–11705.
[10] Ockenden, A., et al., 2021. Towards more ecologically relevant investigations of the impacts of microplastic pollution in freshwater ecosystems. Sci Total Environ 792, 148507.
[11] Rozman, U., Kalčíková, G., 2022. Seeking for a perfect (non-spherical) microplastic particle - The most comprehensive review on microplastic laboratory research. J Hazard Mater 424 (Pt C), 127529.
[12] Connors, K.A., Dyer, S.D., Belanger, S.E., 2017. Advancing the quality of environmental microplastic research. Environ Toxicol Chem 36 (7), 1697–1703.
[13] Sørensen, L., Gerace, M.H., Booth, A.M., 2024. Small micro- and nanoplastic test and reference materials for research: Current status and future needs. Camb Prism Plast 2, e13.
[14] Von Der Esch, E., et al., 2020. Simple generation of suspensible secondary microplastic reference particles via ultrasound treatment. Front Chem 8.
[15] Martínez-Francés, E., et al., 2023. Innovative reference materials for method validation in microplastic analysis including interlaboratory comparison exercises. Anal Bioanal Chem 415 (15), 2907–2919.
[16] Kühn, S., et al., 2018. Marine microplastic: preparation of relevant test materials for laboratory assessment of ecosystem impacts. Chemosphere 213, 103–113.
[17] McColley, C.J., et al., 2023. An assessment of methods used for the generation and characterization of cryomilled polystyrene micro- and nanoplastic particles. Micro Nanoplast 3 (1).
[18] Boettcher, H., Kukulka, T., Cohen, J.H., 2023. Methods for controlled preparation and dosing of microplastic fragments in bioassays. Sci Rep 13 (1).
[19] Maslen, C., et al., 2025. Cryogenic milling of consumer plastics for high-throughput characterization of polydisperse, amorphous microplastics. J Appl Polym Sci.
[20] Zhu, Y.G., et al., 2006. Effect of cryomilling on the thermal behaviors of poly (ethylene terephthalate). J Appl Polym Sci 99 (6), 2868–2873.
[21] Stranz, M., Köster, U., 2004. Irreversible structural changes in cryogenic mechanically milled isotactic polypropylene. Colloid Polym Sci 282 (4), 381–386.
[22] PlasticsEurope, *Plastics – The Fast Facts 2024*. 2024.
[23] da Costa Araújo, A.P., et al., 2020. How much are microplastics harmful to the health of amphibians? A study with pristine polyethylene microplastics and Physalaemus cuvieri. J Hazard Mater 382, 121066.
[24] Zanoni, I., et al., 2025. Characterization of polyethylene and polyurethane microplastics and their adsorption behavior on Cu2+ and Fe3+ in environmental matrices. Environ Sci Eur 37 (1).
[25] Pfohl, P., et al., 2022. Environmental degradation of microplastics: how to measure fragmentation rates to secondary micro- and nanoplastic fragments and dissociation into dissolved organics. Environ Sci Technol 56 (16), 11323–11334.
[26] Folbert, M., Stoorvogel, J., Löhr, A., 2025. Plastic pellet spills and leakages during maritime transportation: a transdisciplinary approach to understand the complex causal pathways. Mar Pollut Bull 218, 118194.
[27] Jonna, S., Lyons, J., 2005. Processing and properties of cryogenically milled post-consumer mixed plastic waste. Polym Test 24 (4), 428–434.
[28] Lievens, S., et al., 2023. A production and fractionation protocol for polyvinyl chloride microplastics. Methods Protoc 6 (1), 15.
[29] Gardon, T., et al., 2022. Cryogrinding and sieving techniques as challenges towards producing controlled size range microplastics for relevant ecotoxicological tests. Environ Pollut 315, 120383.
[30] Heu, R., et al., 2019. Target material selection for sputter coating of SEM samples. Microsc Today 27 (4), 32–36.
[31] Tsuge, S., Ohtani, H., Watanabe, C., 2011. Pyrolysis - GC/MS Data Book of Synthetic Polymers: Pyrograms, Thermograms and MS of Pyrolyzates. Elsevier Science.
[32] De Falco, F., et al., 2023. A thermoanalytical insight into the composition of biodegradable polymers and commercial products by EGA-MS and Py-GC-MS. J Anal Appl Pyrol 171, 105937.
[33] Jones, N., et al., 2021. Analysis of microplastics in environmental samples by pyrolysis/thermal desorption-(GC)xGC-TOFMS. Chromatogr Today 14 (2), 36–40.
[34] Ahmed, A.K., et al., 2017. Crystallization and melting behavior of i-PP: a perspective from Flory's thermodynamic equilibrium theory and DSC experiment. RSC Adv 7 (67), 42491–42504.
[35] Prunier, J., et al., 2019. Trace metals in polyethylene debris from the North Atlantic subtropical gyre. Environ Pollut 245, 371–379.
[36] Turner, A., Filella, M., 2021. Hazardous metal additives in plastics and their environmental impacts. Environ Int 156, 106622.
[37] Kefer, S., Friedenauer, T., Langowski, H.C., 2022. Characterisation of different manufactured plastic microparticles and their comparison to environmental microplastics. Powder Technol 412, 117960.
[38] Astner, A.F., et al., 2019. Mechanical formation of micro- and nano-plastic materials for environmental studies in agricultural ecosystems. Sci Total Environ 685, 1097–1106.
[39] Moura, D.S., et al., 2023. Characterisation of microplastics is key for reliable data interpretation. Chemosphere 331, 138691.
[40] Yuan, Q., et al., 2022. UV-aging of microplastics increases proximal ARG donor-recipient adsorption and leaching of chemicals that synergistically enhance antibiotic resistance propagation. J Hazard Mater 427, 127895.
[41] Schwarzer, M., et al., 2022. Shape, size, and polymer dependent effects of microplastics on Daphnia magna. J Hazard Mater 426, 128136.
[42] Choi, J.S., et al., 2018. Toxicological effects of irregularly shaped and spherical microplastics in a marine teleost, the sheepshead minnow (Cyprinodon variegatus). Mar Pollut Bull 129 (1), 231–240.
[43] Sait, S.T.L., et al., 2021. Microplastic fibres from synthetic textiles: environmental degradation and additive chemical content. Environ Pollut 268 (Pt B), 115745.
[44] Zettler, E.R., Mincer, T.J., Amaral-Zettler, L.A., 2013. Life in the "Plastisphere": microbial communities on plastic marine debris. Environ Sci Technol 47 (13), 7137–7146.
[45] Tewari, A., et al., 2022. Microplastics for use in environmental research. J Polym Environ 30 (10), 4320–4332.
[46] Eitzen, L., et al., 2019. The challenge in preparing particle suspensions for aquatic microplastic research. Environ Res 168, 490–495.
[47] Frias, J.P.G.L., Nash, R., 2019. Microplastics: finding a consensus on the definition. Mar Pollut Bull 138, 145–147.
[48] GESAMP, *Sources, fate and effects of microplastics in the marine environment: a global assessment*. Rep. Stud. GESAMP, ed. P.J. Kershaw. 2015: (IMO/FAO/UNESCO-IOC/UNIDO/WMO/IAEA/UN/UNEP/UNDP Joint Group of Experts on the Scientific Aspects of Marine Environmental Protection).
[49] Wright, S.L., Thompson, R.C., Galloway, T.S., 2013. The physical impacts of microplastics on marine organisms: a review. Environ Pollut 178, 483–492.
[50] Rehse, S., Kloas, W., Zarfl, C., 2016. Short-term exposure with high concentrations of pristine microplastic particles leads to immobilisation of Daphnia magna. Chemosphere 153, 91–99.
[51] Teuten, E.L., et al., 2007. Potential for plastics to transport hydrophobic contaminants. Environ Sci Technol 41 (22), 7759–7764.
[52] Zhou, N., et al., 2023. Size-dependent toxicological effects of polystyrene microplastics in the shrimp Litopenaeus vannamei using a histomorphology, microbiome, and metabolic approach. Environ Pollut 316, 120635.
[53] Ding, T., et al., 2023. Size-dependent effect of microplastics on toxicity and fate of diclofenac in two algae. J Hazard Mater 451, 131071.
[54] Kim, S.A., et al., 2022. Assessing the size-dependent effects of microplastics on zebrafish larvae through fish lateral line system and gut damage. Mar Pollut Bull 185, 114279.
[55] Hrovat, B., et al., 2024. Preparation of synthetic micro- and nano plastics for method validation studies. Sci Total Environ 925, 171821.
[56] Gewert, B., Plassmann, M.M., MacLeod, M., 2015. Pathways for degradation of plastic polymers floating in the marine environment. Environ Sci Process Impacts 17 (9), 1513–1521.
[57] Parker, F.S., 1971. Amides and Amines. In: Parker, F.S. (Ed.), Applications of Infrared Spectroscopy in Biochemistry, Biology, and Medicine. Springer US, Boston, MA, pp. 165–172.
[58] Gulmine, J.V., et al., 2002. Polyethylene characterization by FTIR. Polym Test 21 (5), 557–563.
[59] Höfer, R., Hinrichs, K., 2009. Additives for the Manufacture and Processing of Polymers. In: Eyerer, P., Weller, M., Hübner, C. (Eds.), Polymers - Opportunities and Risks II: Sustainability, Product Design and Processing. Springer Berlin Heidelberg, Berlin, Heidelberg, pp. 97–145.
[60] Gubała, D., et al., 2021. Heads or tails: Nanostructure and molecular orientations in organised erucamide surface layers. J Colloid Interface Sci 590, 506–517.
[61] Sankhe, S.Y., Janorkar, A.V., Hirt, D.E., 2003. Characterization of Erucamide Profiles in LLDPE Films: Depth-Profiling Attempts Using FTIR Photoacoustic Spectroscopy and Raman Microspectroscopy. J Plast Film Sheet 19 (1), 16–29.
[62] SepSolve Analytical Ltd., *Streamlined identification of malodours in recycled plastics with Smart Subtract® [White Paper]*. 2025.
[63] De Frond, H., Rubinovitz, R., Rochman, C.M., 2021. μATR-FTIR Spectral Libraries of Plastic Particles (FLOPP and FLOPP-e) for the Analysis of Microplastics. Anal Chem 93 (48), 15878–15885.
[64] Li, W., et al., 2024. Effect of particle density on microplastics transport in artificial and natural porous media. Sci Total Environ 935, 173429.
[65] Li, Y., et al., 2024. Leaching of chemicals from microplastics: a review of chemical types, leaching mechanisms and influencing factors. Sci Total Environ 906, 167666.
[66] Bridson, J.H., et al., 2021. Leaching and extraction of additives from plastic pollution to inform environmental risk: A multidisciplinary review of analytical approaches. J Hazard Mater 414, 125571.
[67] Boháčková, J., Cajthaml, T., 2024. Contribution of chemical toxicity to the overall toxicity of microplastic particles: a review. Sci Total Environ 957, 177611.
[68] Zimmermann, L., et al., 2020. What are the drivers of microplastic toxicity? Comparing the toxicity of plastic chemicals and particles to Daphnia magna. Environ Pollut 267, 115392.
[69] Mao, R., et al., 2020. Aging mechanism of microplastics with UV irradiation and its effects on the adsorption of heavy metals. J Hazard Mater 393, 122515.
[70] Moura, D.S., et al., 2024. Aging microplastics enhances the adsorption of pharmaceuticals in freshwater. Sci Total Environ 912, 169467.

[71] An, G., et al., 2024. Increased adsorption of diflubenzuron onto polylactic acid microplastics after ultraviolet weathering can increase acute toxicity in the water flea (Daphnia magna). Sci Total Environ 957, 177600.
[72] Liu, Z., et al., 2023. Anionic nanoplastic contaminants promote Parkinson's disease–associated α-synuclein aggregation. Sci Adv 9 (46).
[73] Narayana, R., Mohana, C., Kumar, A., 2022. Analytical characterization of erucamide degradants by mass spectrometry. Polym Degrad Stab 200, 109956.
[74] Shuler, C.A., Janorkar, A.V., Hirt, D.E., 2004. Fate of erucamide in polyolefin films at elevated temperature. Polym Eng Sci 44 (12), 2247–2253.
[75] Altinsoy, A., Arslan, Y., 2022. Investigation of the effects of deep cryogenic treatment on the structural and mechanic properties of polyoxymethylene copolymer (POM-C) materials. Proc Inst Mech Eng Part E 238 (6), 2623–2632.
[76] Ni, H., et al., 2018. Effect of Cryogenic Treatment on Micro-structure and Properties of Different Polymer Materials. MATEC Web Conf 166, 01002.
[77] Akhir, M.A.M., Mustapha, M., 2022. Formulation of biodegradable plastic mulch film for agriculture crop protection: a review. Polym Rev 62 (4), 890–918.
[78] Jiang, L., Wolcott, M.P., Zhang, J., 2006. Study of biodegradable polylactide/poly (butylene adipate-co-terephthalate) blends. Biomacromolecules 7 (1), 199–207.
[79] Stranz, M., Köster, U., Katzenberg, F., 2005. Formation of polymer blends and nano-composites by cryogenic mechanical milling. J Metastab Nanocryst Mater 24-25, 609–614.
[80] Ojijo, V., Ray, S.Sinha, Sadiku, R., 2012. Role of specific interfacial area in controlling properties of immiscible blends of biodegradable polylactide and poly [(butylene succinate)-co-adipate]. ACS Appl Mater Interfaces 4 (12), 6690–6701.
[81] Ducoli, S., et al., 2024. Characterization of polyethylene terephthalate (PET) and polyamide (PA) true-to-life nanoplastics and their biological interactions. Environ Pollut 343, 123150.
[82] Lionetto, F., et al., 2021. Production and characterization of polyethylene terephthalate nanoparticles. Polymers 13 (21), 3745.
[83] Ducoli, S., et al., 2025. Comparison of different fragmentation techniques for the production of true-to-life microplastics. Talanta 283, 127106.
[84] Cuthbertson, A.A., et al., 2024. Characterization of polymer properties and identification of additives in commercially available research plastics. Green Chem 26 (12), 7067–7090.
[85] Hoseini, M., Stead, J., Bond, T., 2023. Ranking the accelerated weathering of plastic polymers. Environ Sci Process Impacts 25 (12), 2081–2091.
[86] Meides, N., et al., 2022. Quantifying the fragmentation of polypropylene upon exposure to accelerated weathering. Micro Nanoplast 2 (1).
[87] ter Halle, A., et al., 2017. To what extent are microplastics from the open ocean weathered? Environ Pollut 227, 167–174.
[88] Zhao, M., et al., 2022. Adsorption of different pollutants by using microplastic with different influencing factors and mechanisms in wastewater: a review. Nanomaterials 12 (13), 2256.
[89] Petrovics, N., et al., 2023. Effect of crystallinity on the migration of plastic additives from polylactic acid-based food contact plastics. Food Packag Shelf Life 36, 101054.
[90] Maghsoud, Z., Rafiei, M., Famili, M.H.N., 2018. Effect of processing method on migration of antioxidant from HDPE packaging into a fatty food simulant in terms of crystallinity. Packag Technol Sci 31 (3), 141–149.
[91] Kobayashi, Y., et al., 2021. Changes in crystal structure and accelerated hydrolytic degradation of polylactic acid in high humidity. Polymers 13 (24), 4324.
[92] Cai, H., et al., 1996. Effects of physical aging, crystallinity, and orientation on the enzymatic degradation of poly (lactic acid). J Polym Sci Part B Polym Phys 34 (16), 2701–2708.
[93] Flint, S., et al., 2012. Bisphenol A exposure, effects, and policy: a wildlife perspective. J Environ Manag 104, 19–34.
[94] Galloway, T.S., et al., 2018. In: Harrison, R.M., Hester, R.E. (Eds.), Plastics Additives and Human Health: A Case Study of Bisphenol A (BPA), in Plastics and the Environment. The Royal Society of Chemistry, pp. 131–155.
[95] Fries, E., et al., 2013. Identification of polymer types and additives in marine microplastic particles using pyrolysis-GC/MS and scanning electron microscopy. Environ Sci Process Impacts 15 (10), 1949–1956.
[96] Peñas, M.I., et al., 2022. A review on current strategies for the modulation of thermomechanical, barrier, and biodegradation properties of poly (butylene succinate) (PBS) and its random copolymers. Polymers 14 (5), 1025.
[97] Aliotta, L., et al., 2022. A brief review of poly (butylene succinate) (pbs) and its main copolymers: synthesis, blends, composites, biodegradability, and applications. Polymers 14 (4), 844.
[98] Savitha, K.S., Kumar, M.Senthil, Jagadish, R.L., 2022. Novel hydrolytically stable Lewis acidic ionic liquid catalyst system for polybutylene succinate (PBS) synthesis. Mater Adv 3 (22), 8132–8136.
[99] Barabanov, A.A., et al., 2021. Propylene polymerization over titanium–magnesium catalysts: The effect of internal and external stereoregulating donors on the number of active centers with different stereospecificity and their reactivity in propagation reaction. J Catal 404, 187–197.
[100] Gadomska-Gajadhur, A., Ruśkowski, P., 2020. Biocompatible catalysts for lactide polymerization—catalyst activity, racemization effect, and optimization of the polymerization based on design of experiments. Org Process Res Dev 24 (8), 1435–1442.
[101] Peng, G., et al., 2023. Metal leaching from plastics in the marine environment: an ignored role of biofilm. Environ Int 177, 107988.
[102] Eriksen, M., et al., 2014. Plastic Pollution in the World's Oceans: More than 5 Trillion Plastic Pieces Weighing over 250,000 Tons Afloat at Sea. PLoS ONE 9 (12), e111913.
[103] Parker, L.A., et al., 2023. Protocol for the production of micro- and nanoplastic test materials. Micro Nanoplast 3 (1).
[104] Capolupo, M., et al., 2020. Chemical composition and ecotoxicity of plastic and car tire rubber leachates to aquatic organisms. Water Res 169, 115270.
[105] Halsband, C., et al., 2020. Car tire crumb rubber: does leaching produce a toxic chemical cocktail in coastal marine systems? Front Environ Sci 8.
[106] Mato, Y., et al., 2001. Plastic resin pellets as a transport medium for toxic chemicals in the marine environment. Environ Sci Technol 35 (2), 318–324.